Available online at www.sciencedirect.com
SCIENCE DIRECT®
Engineering Structures 26 (2004) 471–483
ENGINEERING STRUCTURES
www.elsevier.com/locate/engstruct

Feed-forward control of active variable stiffness systems for mitigating seismic hazard in structures

Nikos G. Pnevmatikos [a], Loukas F. Kallivokas [b], Charis J. Gantes [a,*]

[a] Metal Structures Laboratory, Civil Engineering School, National Technical University of Athens, 42 Patision Street, 100-35 Athens, Greece
[b] Department of Civil Engineering, The University of Texas at Austin, Austin, TX 78712, USA

Received 18 June 2003; received in revised form 13 November 2003; accepted 13 November 2003

Abstract

In this paper we discuss a practical two-stage approach (design and operation) to the seismic control of structures equipped with active variable stiffness (AVS) systems, as a means to mitigate or eliminate resonance or near-resonance phenomena in structures due to seismic ground motion. During the design stage, past seismic events are processed to extract the characteristic frequency content against which the AVS-equipped structure is designed, using a conventional envelope spectrum approach. The motivation for the operation stage builds upon advances in early-warning systems that hold the promise of delivering the expected ground motion waveforms at sites equipped with AVS and at instances just prior to the first wave arrival. The working hypothesis for the operation stage is that notification of the incoming motion will be served to the AVS-equipped site so as to allow for a small but sufficient window for moving the hydraulics of the AVS system to compensate for the frequency content of the arriving seismic signal. Numerical results are presented for both design and operation stages of a prototype building under real past seismic events.

Keywords: Active seismic control; Variable stiffness system; Bracing systems; Resonance control; Early-warning systems

1. Introduction

Active control of seismically excited buildings has attracted considerable attention in recent years. In addition to the long-held desire for designing structures capable of withstanding the effects of strong earthquakes, attention in active control systems is also fuelled by significant advances in both active and passive devices capable of altering the dynamic characteristics of a structure in real- or near-real-time (in this context, real- or near-real-time, refers to the ability to control a structure during the time the seismic ground motion shakes the structure). These advances, coupled with the proliferation of a newer generation of strong motion recorders that result in arrays of increased density over seismic-prone areas (e.g. ANSS—Advance National Seismic System in the US), and with parallel developments in the network infrastructure, computational hardware, and associated computational processing methodologies, bring ever closer the possibility for advanced early-warning systems. Such systems will allow the delivery of the characteristics of the incoming seismic motion prior to the actual wave arrival, thus permitting the tuning of active control devices to the specifics of the actual event, and thereby significantly reducing the potential for catastrophic damage (see e.g. [1] for an implementation of an early-warning system in Taiwan). With these ideas in mind, in this paper we discuss a simple approach for tackling issues related to the design of structures equipped with active control devices focusing on active variable stiffness (AVS) systems, both from a design and an operational perspective.

2. Background

The research and application of active control to civil engineering structures include analytical studies

* Corresponding author. Fax: +30-210-7723442.
E-mail address: chgantes@central.ntua.gr (C.J. Gantes).

0141-0296/$ - see front matter © 2004 Elsevier Ltd. All rights reserved.
doi:10.1016/j.engstruct.2003.11.003

and experimental verifications. The works of Housner et al., Kobori et al., and Spencer et al. are the most representative [2–5]. Several well-established algorithms in control engineering have been introduced to control structures, such as optimal control LQR or LQG [6,7], sliding mode control [8], H_2 and H_∞ [9,10]. The most suitable algorithms for structural application and the practical considerations that should be taken into account are described by Soong [11]. However, due to doubts regarding the effectiveness of the control mechanisms under severe earthquakes, and the limitations of operational energy, relatively few structures are equipped with active control force-type systems, while many more are equipped with passive control systems, which are easier to use and to maintain but have rather limited effectiveness [12,13].

Research on active control systems has primarily focused on the response of force-type systems. Examples include the active mass driver (AMD), which uses the inertia of an auxiliary mass as the control force, and the Active Tendon System, which applies a direct control force by operating an actuator [4,5]. These systems are relatively simple and easy to operate. However, as the structural system becomes more complex and the seismic motion stronger, considerable more energy is required to operate force-type systems. To overcome the energy problem, several hybrid and semi-active systems have been proposed. Examples include the hybrid mass damper (HMD), which is a combination of a passive tuned mass damper (TMD) and an active control actuator [14–16], the semi-active controllable fluid dampers based on electrorheological or magnetorheological fluids [17–22], friction control devices which are used either as energy dissipators within the lateral bracing of a structure or as components within sliding isolation systems [23–27], semi-active viscous fluid dampers [28–33] and stiffness control devices, which are used to modify the stiffness and thus the dynamic characteristics of the structure to which they are attached. The latter systems have been investigated by Kobori et al. [34], Nasu et al. [35], Nemer [36], Loh and Ma [37], Yamada and Kobori [38], Yang et al. [39] and Nagarajaiah [40].

In [35,41–43], Kobori et al. have proposed a non-resonant control system, so-called AVS. This system aims at producing a non-resonant condition during earthquakes by altering the buildings' stiffness based on the characteristics of the earthquake. The stiffness is changed by locking or unlocking certain devices (variable stiffness devices, VSD), which are located between the beams and/or the diagonal braces of a structure. The main advantage of such systems is that the aforementioned energy problem is now satisfactorily addressed, since the VSD can be activated by a small amount of energy. In addition, safety concerns are also mitigated, for such devices do not induce forces, as actuators do (force-type systems): though the possibility of delivering a faulty signal to a VSD system does exist, the activation of a VSD will merely alter the dynamic characteristics of the structure, without, however, inducing secondary vibrations or applying undesirable forces to it.

3. Variable stiffness control based on non-resonance theory

Most response control systems, known as control force-type systems, reduce the structural response by means of a control force, which is regulated by a feed-back algorithm using the measured structural response. On the other hand, the control strategy adopted in the AVS systems is not a feed-back strategy but a feed-forward one, based on non-resonance theory and using only the measured input excitation.

The system dynamics for locking and unlocking VSD systems (e.g. bracings) is highly nonlinear. Hence, control theories for linear systems are not applicable to AVS systems. Kobori and Kamagata [43] suggested a control algorithm to either lock or unlock the bracings in order to shift the building frequencies as far away as possible from the earthquake's dominant frequencies. The main idea of the algorithm was that the bracings should be locked if the product of inter-story drift $x(t)$ and velocity $\dot{x}(t)$ is positive, that is, if $x(t)$ and $\dot{x}(t)$ are in the same direction. By contrast, if $x(t)$ and $\dot{x}(t)$ are opposite to each other, then the bracings should be unlocked.

Another approach suggested by Nasu et al. [35] entails that the response be estimated for each stiffness type in real-time with a motion analyzer, or with a real-time simulator, and calculations be carried out to obtain stiffness selection judgment indices J_i, representing the increasing or decreasing trend of the response of a stiffness type i. Then, the stiffness type i that provides the minimum index J_i is chosen. The algorithm was implemented in a trial building in Japan and showed good performance [35].

Another approach for seismic response control of buildings that are equipped with AVS systems is based on the theory of sliding mode control (SMC). The main feature of the theory of sliding mode control is to design controllers to drive the response trajectory (displacement and velocity) into the sliding surface on which the response trajectory moves stably toward the equilibrium position referred to as the sliding mode. Yang et al. [39] describe how the theory of sliding mode control is applied to structural systems. They also consider the AVS system as an energy dissipation device.

In the present paper, the feed-forward control approach for AVS systems is based on the building's design characteristics relative to the frequency spectrum of the earthquake-induced excitation. In this context, we refer to structures that are characterized by different stiffness (similar to [35]), realized through and dependent upon the selective engagement of the VSD systems; we refer to these discrete and distinct alternatives of a structure's stiffness as stiffness types. First, processing on-the-fly either the entire or an initial part of the incoming earthquake excitation the frequency content of the incoming motion is obtained by the conventional means of real-time fast Fourier transform (FFT). Then, the stiffness type of the building is selected based on the relation between the first eigenfrequency of every stiffness type and the dominant frequencies of the incoming seismic motion. The stiffness type whose first eigenfrequency is farther away from the main frequency window (frequency aperture) of the earthquake is selected. The detailed description of the procedure follows.

4. Methodology outline

The proposed methodology to avoid building resonance consists of two stages—design and operation. In the design stage, the frequency content of a series of prototype earthquakes exhibiting both high and low frequency components is examined, to find out the range of frequencies that contribute to the energy of the expected seismic motion at a given site. These frequencies are candidates to come in resonance with the building, and knowledge of their range will assist in designing the AVS system and make a decision about how many AVS devices should be activated. The issues of pattern selection and of how the AVS will be activated, depending on the specific earthquake, is addressed in the operation stage based on a real-time FFT of either the entire or an initial part of the earthquake record in order to establish the motion's dominant frequencies. Thus, a strategy of how the controller chooses the stiffness type is proposed. In the next sections, the two stages are described in detail.

4.1. Design stage

Let us assume that for a given structure two stiffness types may arise, a soft type I, and a stiff type II (shown schematically in Fig. 1), by deactivating or activating, respectively, the variable stiffness devices attached at the end of the diagonal bracings. Without loss of generality, the procedure described herein can also be applied if more than two stiffness types were to be considered. Let $\mathbf{M}$, $\mathbf{K}$ denote the mass and stiffness matrices of the structure, respectively; then, as usual, solution of the eigenvalue problem described by Eq. (1) for each of the two stiffness types I and II, yields the corresponding first eigenfrequencies f_0^{I}, f_0^{II} and/or

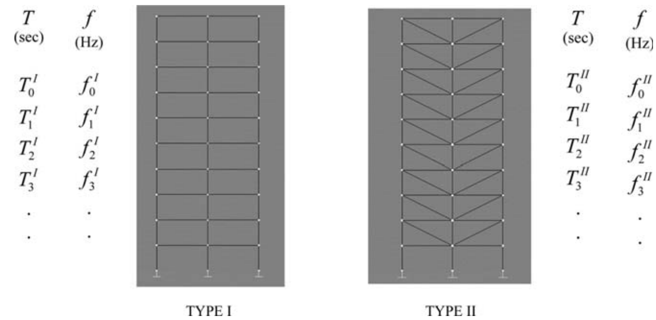

Fig. 1. Stiffness types I (unengaged VSD) and II (engaged VSD) and their respective eigenperiods T_i and eigenfrequencies f_i.

corresponding eigenperiods T_0^{I}, T_0^{II}

$$[\mathbf{K}-\omega^2\mathbf{M}]_{n\times n}\mathbf{\Phi}=0 \Rightarrow |\mathbf{K}-\omega^2\mathbf{M}|=0$$
$$\Rightarrow \omega_0,\omega_1,\ldots,\omega_{n-1} \Rightarrow T_i=\frac{2\pi}{\omega_i},$$
$$f_i=\frac{\omega_i}{2\pi}, \quad i=0,\ldots,n-1, \tag{1}$$

where $\mathbf{\Phi}$ denotes eigenvectors. Since, by construction, type II is stiffer than type I, the following also holds:

$$f_0^{\mathrm{I}}<f_0^{\mathrm{II}}. \tag{2}$$

To describe the design stage, we consider next signals from prototype earthquakes characteristic of the area where the structure will be located. For example, Fig. 2 shows three such records, two from the Athens 1999 earthquake (Fig. 2(a) and (c)) and one from the Mexico City 1985 earthquake (Fig. 2(b)). The first column of Fig. 2 depicts the time signals, whereas the second column depicts the corresponding Fourier-transformed spectra of the entire signal. Clearly, whereas the spectrum of the second record (Fig. 2(b)) shows a very narrow window of dominant frequencies, the corresponding window is wider in the other two records (Fig. 2(a) and (c)). In order to avoid building resonance during the earthquake the condition that should be, at a minimum, satisfied is:

$$f_1,f_2,\ldots f_i \neq f_0^{\mathrm{I}} \quad \text{and} \quad f_1,f_2,\ldots f_i \neq f_0^{\mathrm{II}} \tag{3}$$

where f_i are the dominant spectral frequencies of the earthquake, and f_0^{I}, f_0^{II} are the first frequencies of the two building stiffness types (without and with the VSD systems engaged, respectively). To obtain the f_i, the designer should decide a cut-off value above which the frequencies are considered to contribute significantly to the total earthquake spectrum. This cut-off value or percentage of contribution is defined with respect to the maximum amplitude of the dominant spectrum frequency. That is, if the designer decides to take into account 30% of the maximum amplitude, then all the frequencies with amplitudes more than 30% of the maximum amplitude corresponding to the dominant

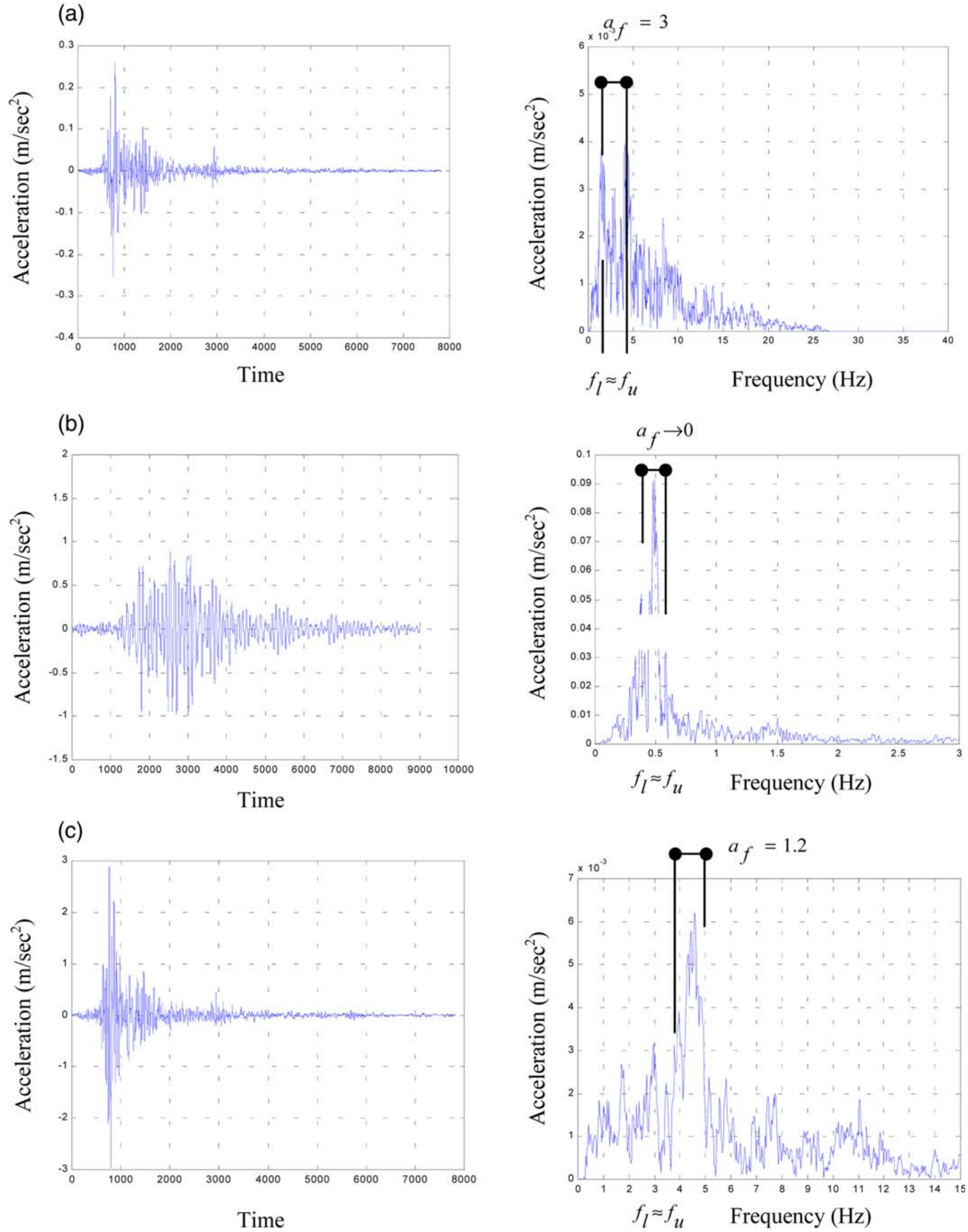

Fig. 2. Three characteristic earthquake signals (first column) and their corresponding spectra (second column); shown is also the range of dominant frequencies (frequency aperture a_f): (a) Athens-1 record and spectrum; (b) Mexico City record and spectrum; (c) Athens-2 record and spectrum.

frequency are considered to contribute significantly to the structure's response. In Fig. 2, the critical percentage of contribution is taken equal to 60%. The higher the cut-off value or critical percentage is, the fewer are the frequencies that are considered to contribute to the signal.

From a design perspective, the inequality in (3) is used in a broad sense and signifies that all f_i should not be in the vicinity of either f_0^{I} or f_0^{II}. Condition (3) should be verified not only for the first natural frequencies of the building but also for the higher modes. This is particularly the case for high-rise buildings, where the higher modes may contribute more to the dynamic response. On the other hand, if the seismic excitation were to create resonance in a building in its fundamental mode, the response will be considerably higher than resonance due to higher modes. This is due to the fact that the participation factors of higher modes are typically much smaller than the participation factors corresponding to the first mode [44,45].

Thus, it is of critical importance, that resonance be avoided, at a minimum, for the fundamental modes, i.e. for the first eigenfrequencies of the corresponding stiffness types I and II. However, by the proposed control procedure it is possible, in some cases, to achieve non-resonance conditions for higher frequencies as well.

Let a_f denote the difference between the upper f_u, and lower f_l bounds of the critical frequency window (henceforth referred to as frequency aperture) of the incoming motion's spectrum (Fig. 2), and let b_f denote the difference between the first eigenfrequencies of the two stiffness types, i.e.:

$$a_f = f_u - f_l \\ b_f = f_0^{II} - f_0^{I} \tag{4}$$

An important condition for the applicability of the proposed decision algorithm is:

$$f_0^{II} > f_u \,||\, f_0^{I} < f_l \tag{5}$$

That is, if resonance is to be avoided, then the natural frequencies of the building stiffness types should fall outside the critical frequency aperture a_f (in (5) "||" denotes an inclusive "or" conditional). We distinguish six such cases for the position of the building's first natural frequencies f_0^{I} and f_0^{II}, corresponding to the unengaged and engaged VSD modes, respectively, relative to the dominant frequency aperture $a_f = f_u - f_l$ of the earthquake spectrum. These cases are schematically summarized in Fig. 3. With the exception of case 4, in all other cases it is possible to avoid resonance phenomena in the fundamental modes by altering the building stiffness type, i.e. by activating the VSD systems. In case 4, both type I and type II fundamental frequencies are within the considered frequency aperture of the earthquake spectrum, and thus resonance cannot be avoided by altering the stiffness type of the structure. If, however, the following condition (6) were to be satisfied at the design stage, then case 4 will also be avoided:

$$a_f < b_f \tag{6}$$

By analyzing more than 50 earthquake records and using a critical percentage of significant contribution equal to 50% (cut-off value), the range of the a_f parameter has been found to vary between 0.1 Hz (for earthquakes dominated by a narrow frequency aperture) and 8 Hz (e.g. Northridge 1994 earthquake). This information is used in selecting the number and section of braces in such a way that b_f is always larger than a_f, by, for example, choosing stiffer bracings.

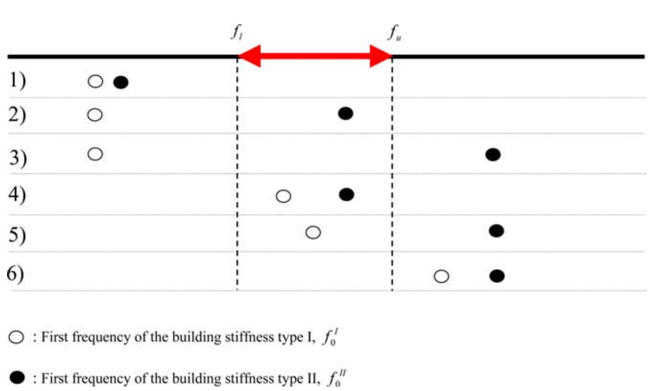

Fig. 3. Matrix of possible cases of the relative position of the difference of the first building natural frequencies b_f between each stiffness type with respect to the frequency aperture a_f of the earthquake spectrum.

4.2. Operation stage

As outlined, the steps taken during the design stage ensure that the VSD systems are capable of altering a structure's natural frequencies by exploiting prior information, that is, by taking into account the frequency content of past events. However, the selective engagement of the VSD systems allow for the fine tuning of a structure's dynamic properties in near-real-time by exploiting the characteristics of the actual seismic event. We envision two separate scenarios under which such tuning can take place: first, by taking into account the sampled waveforms in the near-field, that is, near the epicenter of the event and away from the controlled structure's site (e.g. 40–150 km from the epicenter). Such records will not account for soil amplification effects, or more generally, for the signal filtering that the propagation of the waves through the soil will induce. In general, it is quite possible that one may observe amplification of the original signal at frequencies corresponding to the natural frequencies of the soil medium (layered or not), and possibly simultaneously, de-amplification of the original signal's dominant frequencies (the latter is less frequent, but has been observed (Mexico City 1985 earthquake)). However, for many events, the dominant frequency characteristics of the waveforms close to the epicenter will still survive the soil filtering, and thus the information contained in the near-field records could still be used to tune the VSD systems. In this scenario, what remains to be done is for the near-field waveforms to be communicated to the control site. The latter calls for an implementation of an early-warning system (à la [1]) that will exploit the presence of the networking infrastructure to communicate the waveforms to the control site at speeds higher than the evolving seismic front, thereby allowing for a sufficient window for on-site processing (extraction of the frequency spectrum for activating/tuning of the control devices).

In the second scenario, we do not rely on the near-field records: rather, we exploit records at sites between the epicenter and the control site, where the soil amplification effects may now be, to a large extent, accounted for (we assume that the soil variability between the recording and the control site is minimal). By closing the distance between the recording and control site we also run the risk of not having the benefit of the complete waveforms for analysis purposes due to time-constraints (the waveforms will still have to be communicated to the control site). However, as shown in Fig. 4, it may be sufficient to process (through FFT) only an initial part of the record (possibly up to times that include the S-wave arrival) in order to recover the dominant frequency aperture a_f. In Fig. 4, for example, it is shown that the dominant frequencies of one-eighth, one-quarter, and one-half of the signal of the Mexico City record are approximately the same as the dominant frequencies recovered from processing the entire signal. The same conclusions can be drawn for the Athens-1 and Athens-2 records.

We further note that, as it was shown in [46], the frequency content of the ground motion at a particular site may change during the event duration. Thus, processing of an initial part of the incoming signal may not allow for the correct capture of the dominant frequency aperture a_f. Such a failure will subsequently not allow for the on-the-fly tuning of the VSD systems. With the current density of deployed stations in seismic-prone areas this remains a distinct possibility. However, we expect that as the investment in networked recording stations increases, it would still be possible to resort to the outlined second scenario that will allow for near-real-time processing of the entire (rather than just a part of) incoming signal at sufficient distance from the controlled site and thus the timely notification of the VSD systems prior to the waves arrival.

As the frequency spectrum (through FFT) of either the near-field record or of an initial part of the incoming signal is recovered, then the frequency aperture a_f is known and a decision on which stiffness type to choose can be made. The building is normally held in stiffness type II (stiffest mode, fully engaged VSD), and its stiffness may change according to the following procedure.

If the upper frequency f_u of the incoming signal is smaller than the first frequency of the stiffness type II f_0^{II}, then stiffness type II is chosen (cases 3, 5, 6). If this is not true, then the lower frequency f_l of the frequency aperture is compared against the first frequency of stiffness type I f_0^{I}. Accordingly, if $f_0^{\mathrm{I}} < f_l$, then the stiffness type I is chosen (cases 1 or 2). The decision process is described in the flow chart of Fig. 5, where selected cases in support of the decision algorithm are also shown. Furthermore, in three cases (3, 5 and 6) resonance in the higher modes is also avoided, as can be seen from Figs. 3 and 5. We remark that the overall time needed for earthquake data collection, processing, network propagation, and the stiffness selection algorithm is in the order of few seconds (depends on the event's duration, on distance from the epicenter or the recording site, network congestion and latency, computational hardware, etc.), which we expect that it will not affect the robustness and stability of the proposed scheme.

5. Examples and numerical experiments

5.1. Design stage

Using the outlined process, a ten-story, five-bay, steel frame, with the details as shown in Fig. 6, was analyzed under a base motion corresponding to the three earthquakes. Two stiffness types were chosen, the first type being a frame with all braces open, and the second type with all braces closed. Before the analysis a large of number of both far- and near-field past records should be considered to ensure that their a_f parameter is less than the b_f parameter of the structure, as per condition (6).

As it can be seen from Fig. 2, the spectra of the two records from the Athens and the Mexico City earthquakes have different frequency content. For the prototype signals depicted in Fig. 2, the values of the two design parameters are as follows: in the Mexico City case (Fig. 2(b)), a_f is almost zero, since both the lower and upper frequency bounds are equal to 0.5 Hz; from the spectrum of the Athens-1 record (Fig. 2(a)) a_f is equal to 3 Hz, while the lower and upper bounds are 1.8 Hz and 4.8 Hz, respectively; from the spectrum of the Athens-2 record (Fig. 2(c)) a_f is equal to 1.2 Hz, while the corresponding bounds are 3.8 Hz and 5 Hz, respectively. The characteristics are summarized in Table 1 below. The cross-sectional properties of the braces were chosen such that $b_f = 4.61\ \mathrm{Hz} - 1.08\ \mathrm{Hz} = 3.53\ \mathrm{Hz}$, which is larger than the a_f parameter of the three earthquakes of Fig. 2, which, as outlined is a key decision in the design stage.

5.2. Operation stage

The displacement and acceleration at the top of the buildings with stiffness types I and II are shown in Figs. 7–9 for the entire signals of the Athens-1, Mexico City and Athens-2 records, respectively. The building is initially held in stiffness type II, which is the stiffest. If the proposed algorithm is used then in the case of the Athens-1 earthquake the upper frequency bound $f_u = 4.8$ Hz is near but higher than the first frequency of type II $f_0^{\mathrm{II}} = 4.609$ Hz and therefore stiffness type I is chosen. This corresponds to case 2 of the decision chart of Fig. 3. As it can be seen from Fig. 7, the stiffness type I results in considerably smaller accelerations

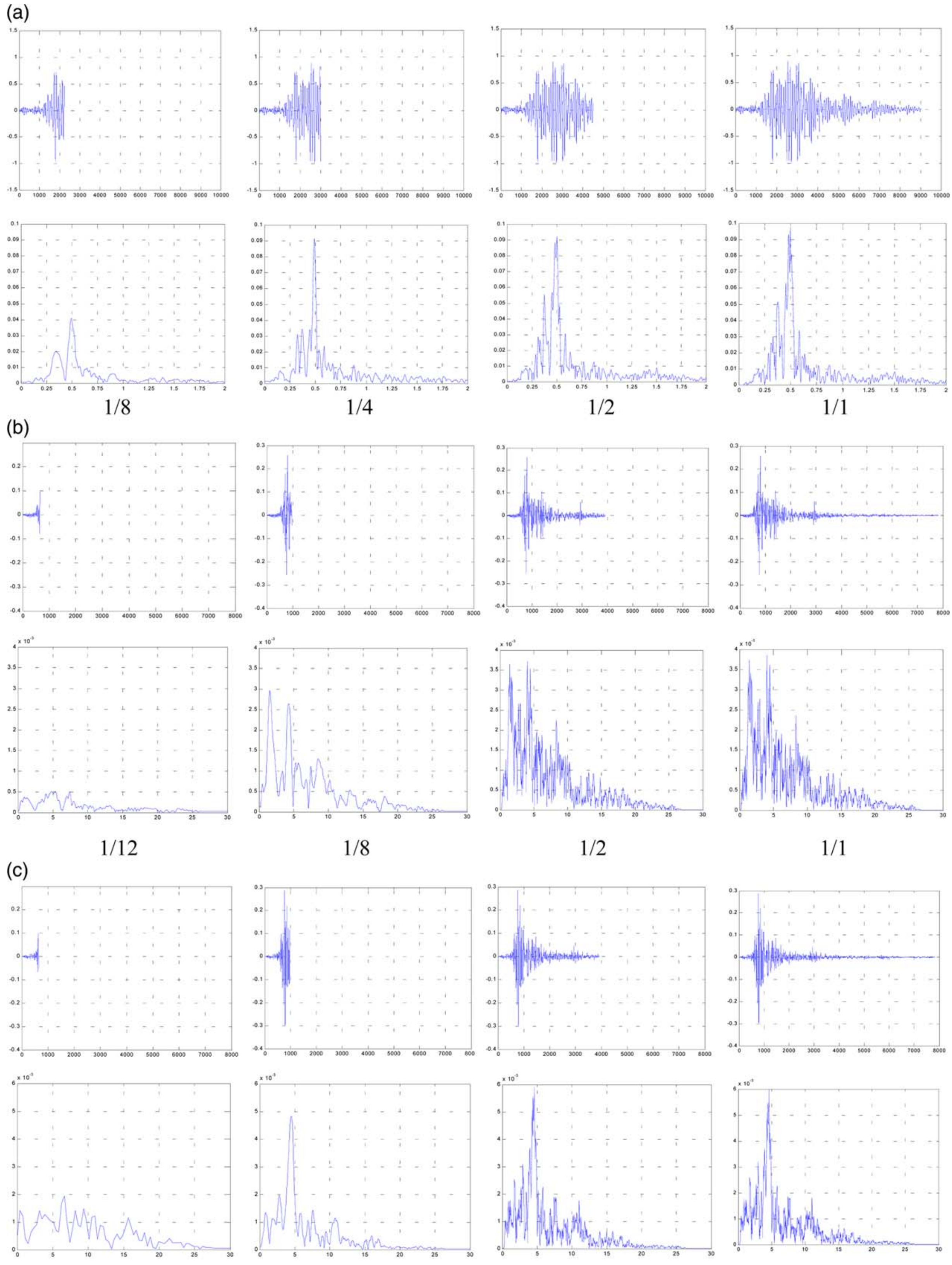

Fig. 4. Acceleration records and corresponding spectra of the entire signal and of initial parts of it from the three earthquakes: (a) Mexico City record; (b) Athens-1 record; (c) Athens-2 record.

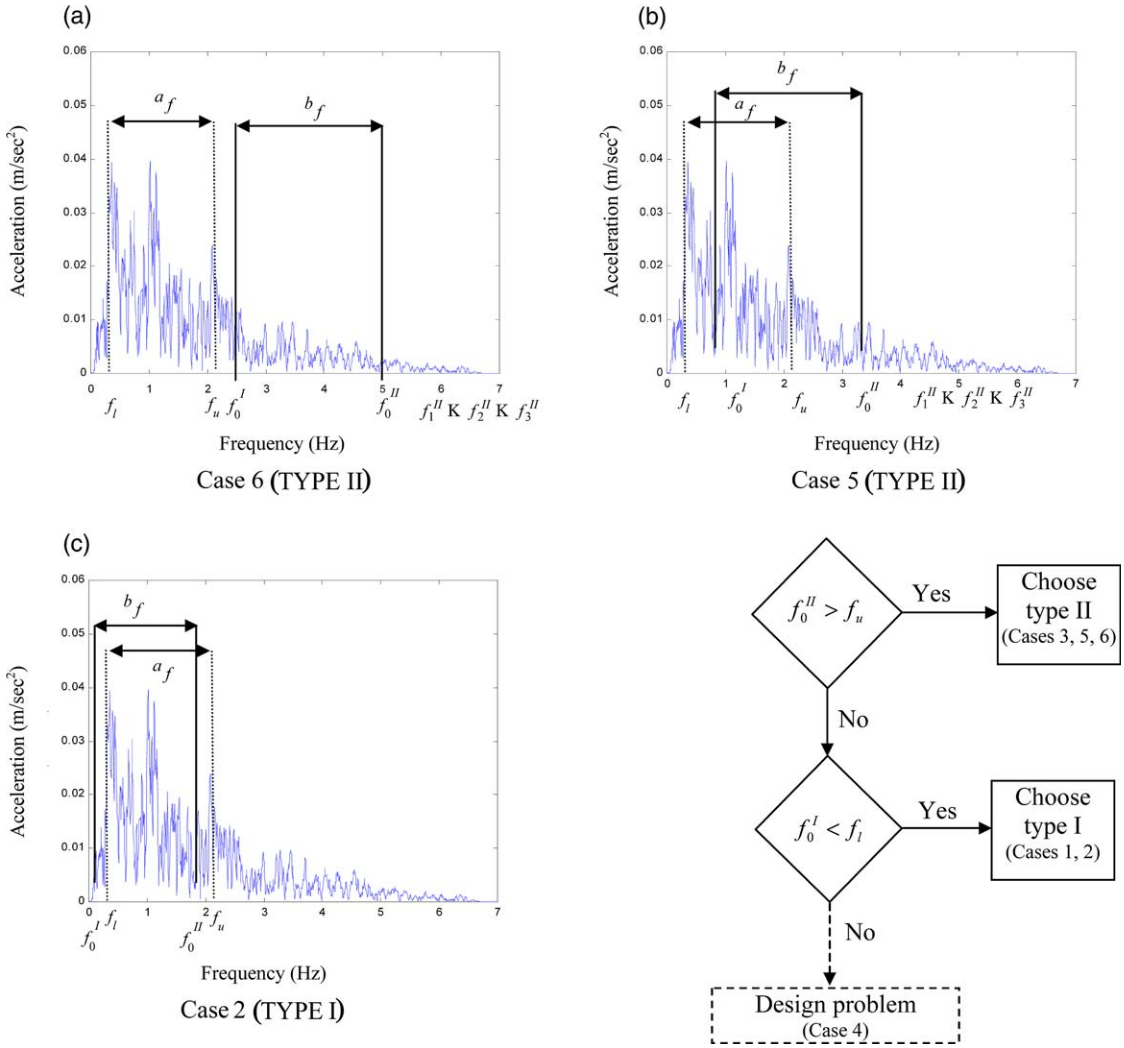

Fig. 5. Decision support flow chart for building stiffness types; relative placement of the frequency aperture a_f and the building frequencies b_f and the corresponding decision.

than the stiffness type II (the peak value is reduced by a factor of 3.5). The incoming motion's spectrum frequency aperture, which is obtained by real time FFT, is compared in real time to the first frequencies of each stiffness type (1.08 Hz and 4.60 Hz, respectively) and the decision is updated.

The use of the above algorithm in the case of the Mexico City record will lead to choosing stiffness type II since the higher frequency (0.5 Hz) of the signal is lower than the first frequency of both type I and type II. This type gives the smaller response (acceleration and displacement) as can be seen from Fig. 8. This case corresponds to case 6 of the decision chart of Fig. 3. Finally, if the above algorithm is used in the case of Athens-2 earthquake, the record's upper frequency, 5.0

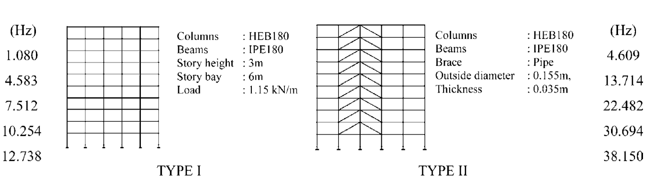

Fig. 6. Stiffness types I and II and their corresponding eigenfrequencies.

Table 1
Frequency aperture and bounds for three prototype seismic events

Records	Frequencies		
	f_l (Hz)	f_u (Hz)	a_f (Hz)
Athens-1	1.8	4.8	3.0
Mexico City	0.5	0.5	0.0
Athens-2	3.8	5.0	1.2

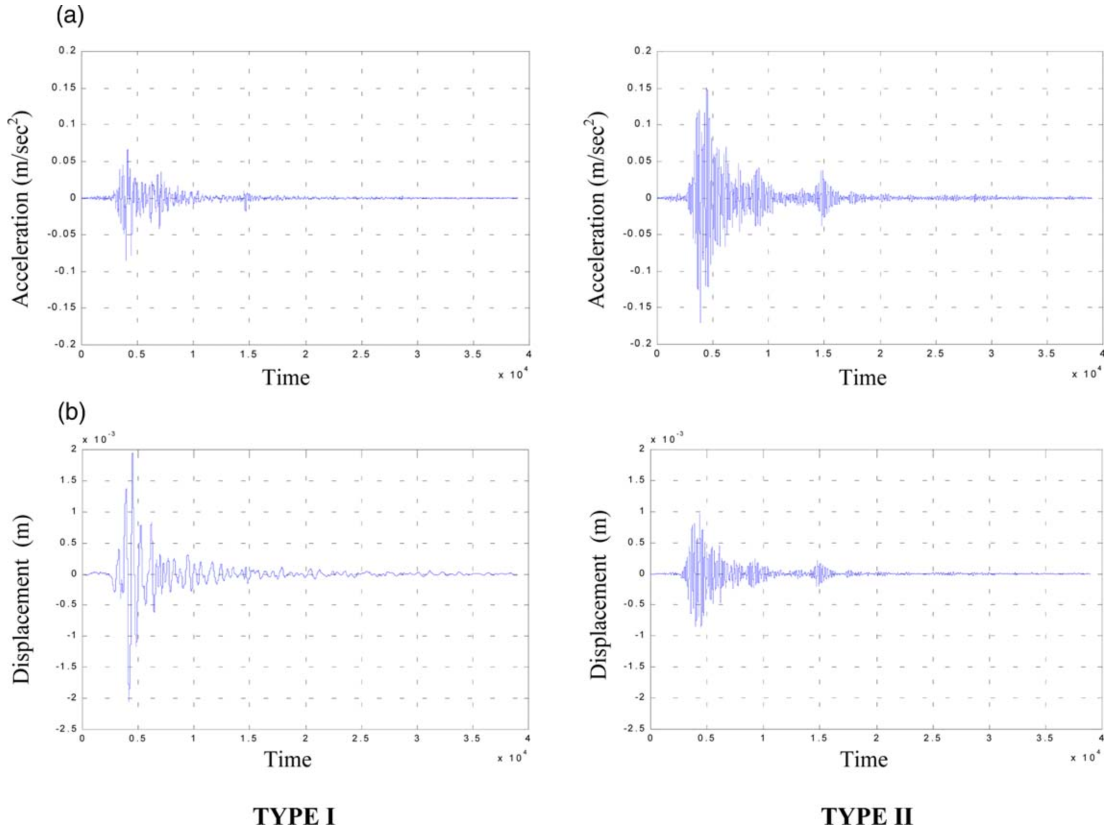

Fig. 7. (a) Top acceleration; and (b) top displacement for the two stiffness types due to the Athens-1 earthquake.

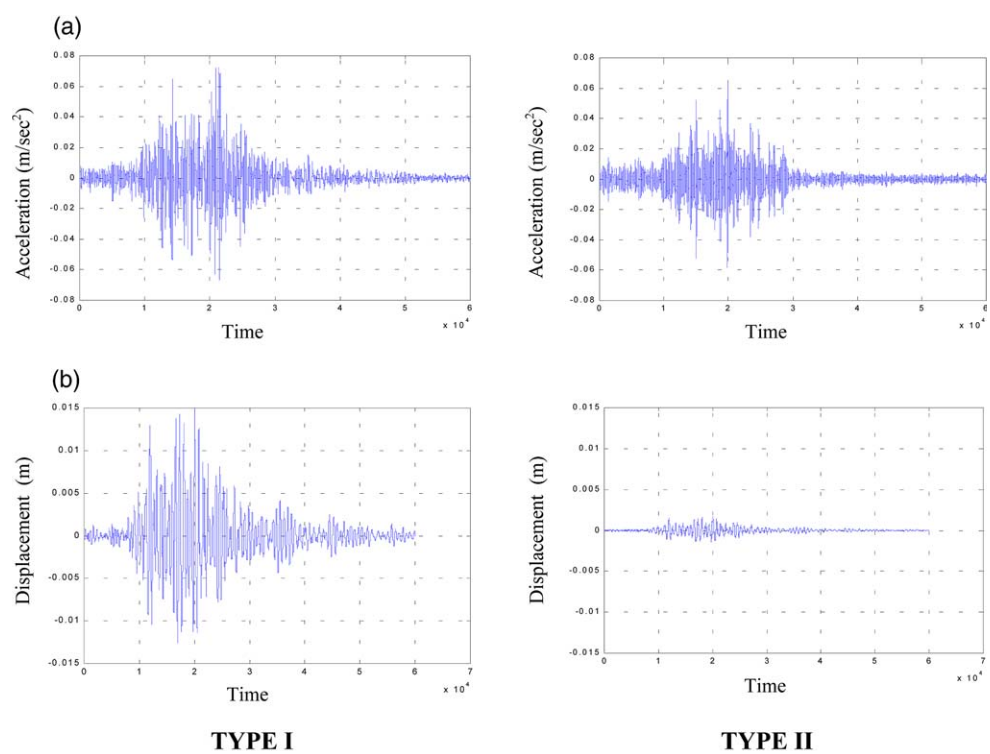

Fig. 8. (a) Top acceleration; and (b) top displacement for the two stiffness types due to the Mexico City earthquake.

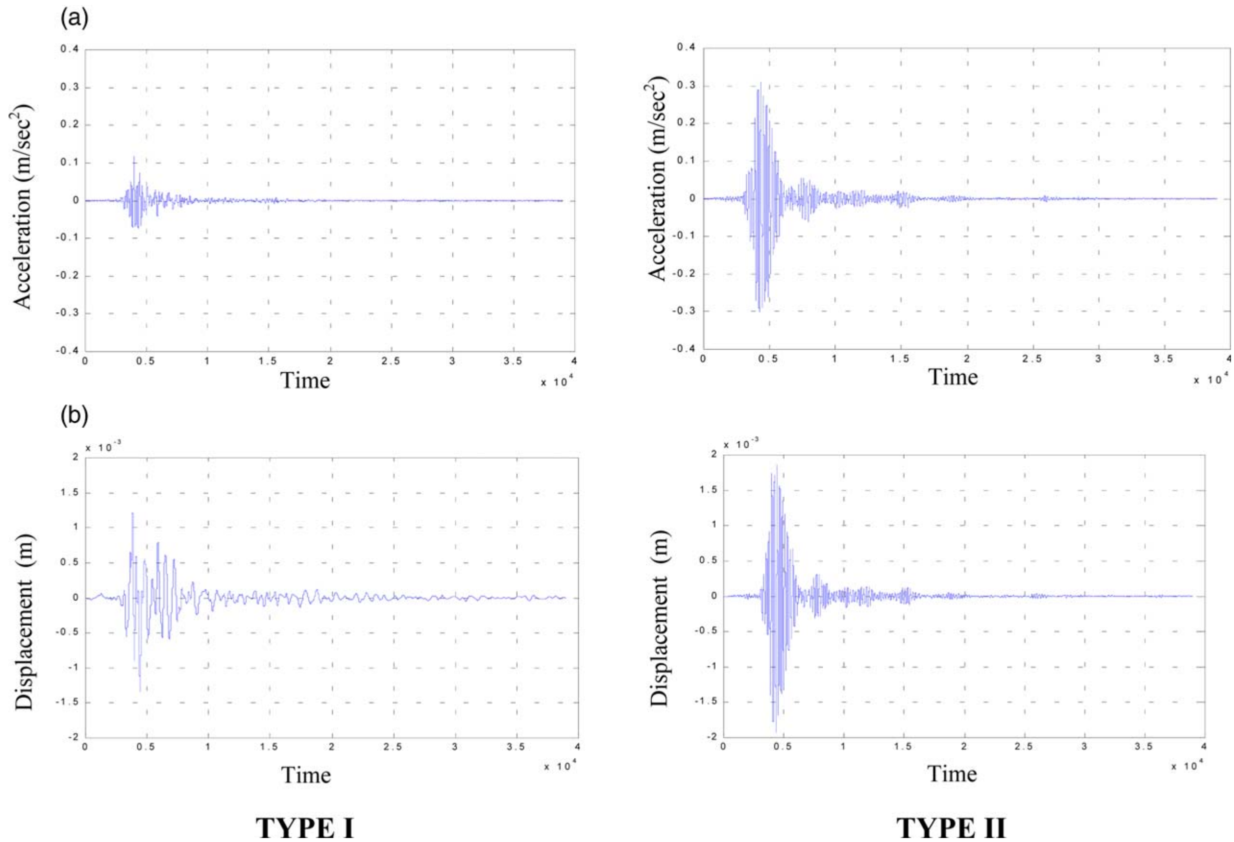

Fig. 9. (a) Top acceleration; and (b) top displacement for the stiffness types due to the Athens-2 earthquake record.

Hz, is higher than the first frequencies of each of the two stiffness types and the stiffness type I would be chosen. As it can be seen from Fig. 9 this type results in lower acceleration and displacement (this case corresponds again to case 2 of Fig. 3).

We remark that, usually, the building is held in the stiffer type II. We expect that there will be sufficient time to allow for a stiffness-type decision prior to the actual arrival of the first wave based on our hypothesis of an early-warning system; however, even if the decision is delayed and the locking or unlocking of the VSD systems extends into the actual motion time experienced at the site by an amount of time equal to t_0 the outlined procedure still holds. To illustrate, consider, for example, the cases of the Athens-1 and Athens-2 records, where, ultimately, the softer stiffness type I is chosen. The total behavior consists of two parts. In the first part (time 0–t_0), where t_0 accounts for all delays between the first wave arrival and the moment the decision to switch type is made, the building behaves as type II and the response of the system is the response of the stiffness type II. In the second part, from time t_0 until the end of the excitation, the building behaves as type I and the response of the system is the response of stiffness type I with initial conditions the end state of the first part. The two parts and the total response (acceleration) at the top of the frame from the Athens-1 record are shown in Fig. 10.

6. Summary and conclusions

A feed-forward control decision strategy based on AVS systems for seismically excited buildings has been presented. The proposed strategy consists of two stages. In the first stage (design), the selection of location and section of braces is made. In the second stage (operation), real time FFT of the incoming signal is performed and a decision procedure for selecting the appropriate stiffness type to avoid resonance is carried out. Simulation results indicate that the response of the building using a VSD system with the proposed activation process is reduced. The advantage of this system is the small amount of energy required. The time interval for data collection, processing, and the decision process is estimated in the order of a few seconds. To verify the numerical simulation results experiments implementing the above control algorithm should be carried out.

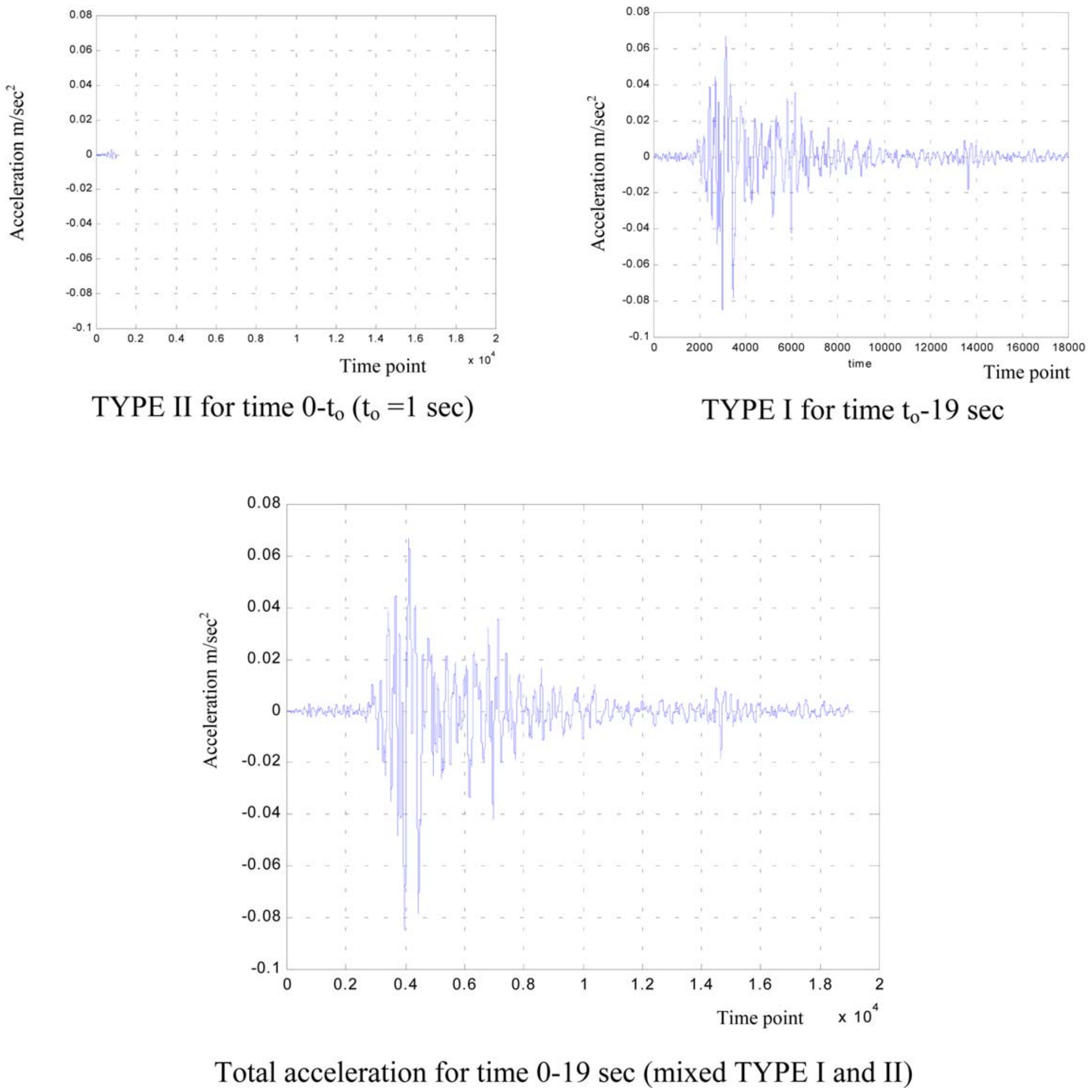

Fig. 10. The two parts and the total top acceleration of the frame due to the Athens-1 record: initial part of the record, up to t_0, corresponds to Type II response, latter part corresponds to Type I (switched) response.

Acknowledgements

The first author wishes to acknowledge the financial support provided by the Greek Scholarship Foundation (IKY).

Appendix Notation

M mass matrix of the structure
K stiffness matrix of the structure
T_0^{I} first eigenperiod of stiffness type I
T_0^{II} first eigenperiod of stiffness type II
f_0^{I} first eigenfrequency of stiffness type I
f_0^{II} first eigenfrequency of stiffness type II
$\boldsymbol{f_i}$ set of dominant frequencies that contribute to the earthquake signal
$\boldsymbol{f}_{\mathrm{u}}$ dominant frequency upper bound
$\boldsymbol{f}_{\mathrm{l}}$ dominant frequency lower bound
$\boldsymbol{a}_{\mathrm{f}}$ frequency aperture
$\boldsymbol{b}_{\mathrm{f}}$ difference in the fundamental frequencies of building stiffness types I and II

References

[1] Wu YM, Teng TL. A virtual subnetwork approach to earthquake early warning. Bulletin of the Seismological Society of America 2002;92(5):2008–18.

[2] Housner GW, Marsi SF, Chassiakos AG. Proceedings of the First World Conference on Structural Control, CA. 1994.

[3] Kobori T, Inoue Y, Seto K, Iemura HN, Nishitani A. Proceedings of the Second World Conference on Structural Control, New York. 1998.

[4] Spencer BF, Dyke SJ, Deoskar HS. Benchmark problem in structural control, Part I: active mass driver system. Proceedings of the ASCE Structures Congress, Portland. 1997.

[5] Spencer BF, Dyke SJ, Deoskar HS. Benchmark problem in structural control, Part II: active tendon system. Proceedings of the ASCE Structures Congress, Portland. 1997.

[6] Yang JN. Application of optimal control theory to civil engineering structures. Journal of Engineering Mechanics Division ASCE 1975;101:819–38.

[7] Abdel-Rohman M, Leipholz H, Quintana VH. Optimal control of civil engineering structures. Journal of Engineering Mechanics Division ASCE 1980;106:57–73.

[8] Yang JN, Wu JC, Agrawal AK, Hsu SY. Sliding mode control of seismically excited linear structures. Journal of Engineering Mechanics ASCE 1995;121:1386–90.

[9] Jabavi F, Schmitendorf WE, Yang JN. H_∞ control for seismic-excited building with acceleration feedback. Journal of Engineering Mechanics ASCE 1995;121:994–1002.

[10] Zacharenakis EC, Arvanitis KG, Soldatos AG, Stavroulakis GE. LQR and H_∞ optimal structural control in aseismic design. Proceedings of the National Mechanics Congress, Thessaloniki. 2001, p. 240–5.

[11] Soong TT. Active structural control: theory and practice. London, New York: Longman Scientific and Technical/Wiley; 1990.

[12] Kobori T. Proceedings of the Second World Conference on Structural Control. Mission and perspective towards future structural control research, vol. 1. 1998, p. 25–34.

[13] Sakamoto M. Applications of structural response control (reviews from the past and issues towards the future). Proceedings of the Second International Workshop on Structural Control. 1996, p. 470–81.

[14] Higashino M, Aizawa S. Application of active mass damper system in actual buildings. In: Housner GW, Marsi SF, editors. Proceedings of the International Workshop on Structural Control, Los Angeles, CA. 1993, p. 194–205.

[15] Soong TT, Reinhorn AM, Aizawa S, Higashino M. Recent structural applications of active control technology. Journal of Structural Control 1994;1(2):5–21.

[16] Chunxiang L, Yanxia L. Active multiple tuned mass dampers for structures under the ground acceleration. Earthquake Engineering and Structural Dynamics 2002;31:1041–52.

[17] Erhrogott RC, Marsi SF. Structural control applications of an electrorheological device. Proceedings of the International Workshop on Structural Control, Honolulu. 1993, p. 115–29.

[18] Gavin HP, Hanson RD, Filisco FE. Electrorheological dampers, Part I: analysis and design. Journal of Applied Mechanics 1996;63:669–75.

[19] Gavin HP, Hanson RD, Filisco FE. Electrorheological dampers, Part II: testing and modeling. Journal of Applied Mechanics 1996;63:676–82.

[20] Makris N, Hill D, Burton S, Jordan M. Proceedings of the Smart Structures and Materials, San Diego, CA. Electrorheological fluid damper for seismic protection of structures, vol. 2443. 1995, p. 184–94.

[21] Spencer BF, Dyke SJ, Sain MK, Carlson JD. Phenomenological model for magnetorheological dampers. Journal of Engineering Mechanics 1997;123(3):230–8.

[22] Dyke SJ, Spencer BF, Sain MK, Carlson JD. Modeling and control of magnetorheological dampers for seismic response reduction. Smart Materials and Structures 1996;5:565–75.

[23] Akbay Z, Aktan HM. Actively regulated friction slip braces. Proceedings of the Sixth Canadian Conference on Earthquake Engineering, Toronto, Canada. 1991, p. 427–35.

[24] Feng MQ, Shinozuka M. Experimental and analytical study of a hybrid isolation system using friction controllable sliding bearings. Report No 92-0009, National center for earthquake engineering Research, Buffalo, NY, 1992.

[25] Dowdell DJ, Cherry S. Proceedings of the First World Conference on Structural Control, Los Angeles, CA. Structural control using semi-active friction dampers, FA1. 1994, p. 59–68.

[26] Fujita T, Shimazaki M, Yutaka H, Aizawa S, Higashino M, Haniuda N. Semi-active seismic isolation system using controllable friction damper. Bulletin of Earthquake Resistant Structure Research Center 1994;27:21–31.

[27] Yang J, Agrawal A. Semi-active hybrid control systems for nonlinear buildings against near-field earthquakes. Engineering Structures 2002;24:271–80.

[28] Patten WN, Kuo CC, He Q, Liu L, Sack RL. Proceedings of the First World Conference on Structural Control, Los Angeles, CA. Seismic structural control via semiactive hydraulic actuators, FA2. 1994, p. 83–9.

[29] Symans MD, Constantinou MC, Taylor DP, Garnujost KD. Proceedings of the First World Conference on Structural Control, Los Angeles, CA. Semi-active fluid viscous dampers for seismic response control, FA4. 1994, p. 3–12.

[30] Symans MD, Constantinou MC. Seismic testing of a building structure with a semi active fluid damper control system. Earthquake Engineering and Structural Dynamics 1997;26:759–77.

[31] Kurata N, Koboti T, Takahahi M, Niwa N, Kurino H. Proceedings of the First World Conference on Structural Control, Pasadena, CA. Shaking table experiment of active variable damping system, TR2. 1994, p. 102–17.

[32] Polak E, Meeker G, Yamada K, Kurata N. Evaluation of an active variable damping structure. Earthquake Engineering and Structural Dynamics 1994;23:1259–74.

[33] Loh C, Ma M. Control of seismically exited building structures using variable damper systems. Engineering Structures 1996;18(4):279–87.

[34] Kobori T, Takahashi M, Nasu T, Niwa N, Ogasawara K. Seismic response controlled structure with active variable stiffness system. Earthquake Engineering and Structural Dynamics 1993;22:925–41.

[35] Nasu T, Kobori T, Niwa N, Ogasawara K. Active variable stiffness system with non-resonant control. Earthquake Engineering and Structural Dynamics 2001;30:1597–614.

[36] Nemer DC, Lin Y, Osegueda RA. Semiactive motion control using variable stiffness. Journal of Structural Engineering 1994;22:925–41.

[37] Loh C, Ma M. Proceedings of the First World Conference on Structural Control, Los Angeles, CA. Active damping or active stiffness control for seismic excited buildings, TA2. 1994, p. 11–20.

[38] Yamada K, Kobori T. Control algorithm for estimating future responses for active variable stiffness structure. Earthquake Engineering and Structural Dynamics 1995;24:1085–99.

[39] Yang JN, Wu JC, Li Z. Control of seismic excited buildings using active variable stiffness. Engineering Structures 1996;18:589–96.

[40] Nagarajaiah S. Semi active control of structures. Proceedings of the Structures Congress XV, ASCE, Portland, OR. 1997, p. 1574–8.

[41] Kobori T. New philosophy of aseismic design—approach on dynamic intelligent building system. Proceedings of the Annual Meeting of Architectural Institution of Japan. 1986, p. 837–8.

[42] Kobori T. Experimental study on active variable stiffness system—active seismic response controlled structure. Proceedings of the Fourth World Congress Council on Tall Buildings and Urban Habitat. 1990, p. 561–72.

[43] Kobori T, Kamagata S. Active variable stiffness system—active seismic response control. In: Housner GW, Marsi SF, Casciati F, Kameda H, editors. Proceedings of the US–Italy–Japan Workshop/Symposium on Structural Control and Intelligent Systems. 1992, p. 140–53.
[44] Clough RW, Penzien J. Dynamics of structures, 2nd ed. McGraw Hill; 1993.
[45] Chopra AK. Dynamics of structures: theory and applications to earthquake engineering. Upper Saddle River, New Jersey: Prentice Hall, 2001.
[46] Saragoni GR, Hart GC. Simulation of artificial earthquakes. Earthquake Engineering and Structural Dynamics 1974;2:249–67.